

Resonance Raman Characterization of Soluble Guanylate Cyclase Expressed from Baculovirus[†]

Baochen Fan,[‡] Gopa Gupta,[§] Robert S. Danziger,[§] Joel M. Friedman,[‡] and Denis, L. Rousseau^{*,‡}

Department of Physiology and Biophysics, Albert Einstein College of Medicine, 1300 Morris Park Avenue, Bronx, New York 10461, and Columbia University, College of Physicians & Surgeons, 630 West 168th Street, New York 10032

Received August 6, 1997; Revised Manuscript Received November 12, 1997

ABSTRACT: Resonance Raman spectra of the $\alpha_1\beta_1$ isoform of bovine lung soluble guanylate cyclase expressed from baculovirus have been measured. The spectra show that the ferric heme is five-coordinate high spin whereas the ferrous heme in the absence of added exogenous ligands is a mixture of six-coordinate low spin and five-coordinate high spin. In the Fe–CO-derivative, the correlation between the Fe–CO frequency (497 cm^{-1}) and the C–O frequency (1959 cm^{-1}) demonstrates that the proximal ligand in our preparation is histidine. The Fe–NO stretching frequency (found at 520 cm^{-1}) and other spectral features of the ferrous Fe–NO-bound sGC are similar to those reported by Deinum et al. (1) and Yu et al. (2). These data indicate that although large preparation-dependent differences in the occupancy of the distal pocket exist, all the preparations have the same proximal histidine ligation and share the same mechanism of activation by NO.

Guanylate cyclase (GC) catalyzes the transformation of GTP to cGMP, a primary signaling molecule in biological systems (3–5). The enzyme has been separated into two general classes, particulate (pGC) and soluble (sGC) forms. In addition to the differences in location in the cells, important differences also exist in the activation mechanism within these classes. The isoforms of pGC are activated by a variety of peptides (6, 7). On the other hand, sGC is activated by small ligands that directly bind to the heme cofactor of the enzyme (8). At present, sGC is the only enzyme that has been identified which is activated by nitric oxide (NO). Coordination by NO to sGC can elevate the enzymatic activity up to 400-fold above the basal level (9, 10). Other molecular species, called guanylate cyclase activating factors, including carbon monoxide (CO) and hydroxide ion (OH^-), have also been observed to activate the enzyme to a certain degree (11).

sGC is a heterodimer composed of two highly homologous subunits: α_1 with a mass of $\sim 80\text{ kDa}$ and β_1 with a mass of $\sim 70\text{ kDa}$ (12, 13). Four different cDNA clones encoding sGC subunits have been obtained (α_2 and β_2 in addition to α_1 and β_1) (5). Although the $\alpha_1\beta_1$ isozyme is the only species isolated from tissue, heterodimers with different subunit combinations also show activity toward cGMP synthesis (14). However, since α_1 and β_1 are detected ubiquitously in tissue, the $\alpha_1\beta_1$ complex is viewed as the physiologically active form of the enzyme. The physiological role of the other subunits remains to be determined.

Recent studies indicate that both subunits, α_1 and β_1 , bind protoporphyrin IX as a prosthetic group (15–17). The heme is presumed to be ligated to a histidine residue as its proximal ligand just as in hemoglobin and myoglobin. However, the ligand binding properties of sGC are quite distinct from other heme proteins with the same axial coordination and prosthetic group. The O_2 and CO affinities are very low due to very high off-rates (18). A structural study of the heme pocket of this unique protein will be important for understanding the structure and functionality of the enzyme and its relation to other heme proteins. It is generally believed that activation of the enzyme, brought about by NO, is due to NO coordination to the heme followed by breakage of the iron–histidine bond. The structural changes initiated by this event propagate through the protein bringing about the conformational changes that lead to its enzymatic activity (2, 4, 8).

Differences between enzymes isolated by different groups and procedures have been clearly demonstrated. In studies by Marletta and co-workers, the enzyme was isolated from bovine lung by a procedure in which the heme prosthetic group is retained during purification. Both the ferric and the ferrous heme in this enzyme were demonstrated to be five-coordinate high spin from several physical measurements (1, 9, 18, 19). In another series of studies by Burstyn and co-workers, the protein was also isolated from bovine lung but in a heme-deficient form and was subsequently reconstituted with protoporphyrin-IX. It was shown that the heme of the enzyme is a mixture of five-coordinate high spin and six-coordinate low spin in this preparation (2, 17, 20). In all cases, the enzyme showed substantial activation by NO. CO shows only a minimal activation of the enzyme, varying from 1-fold to 4-fold over the basal level.

Resonance Raman scattering is a powerful technique to study the properties of heme proteins. It has provided unique insights about the structure of heme active sites due to its

[†] This work was supported by National Institutes of Health Grant GM54806 to D.L.R.

* Corresponding author: Department of Physiology and Biophysics, Albert Einstein College of Medicine, 1300 Morris Park Avenue Bronx, NY 10461. Phone: 718-430-4264. Fax: 718-430-8819. E-mail: Rousseau@Aecom.yu.edu.

[‡] Albert Einstein College of Medicine.

[§] Columbia University.

sensitivity to the spin state and coordination state and protein perturbations on them (21). Previously, the technique has been used to characterize the structure of the heme moiety of soluble guanylate cyclase isolated by both procedures (1, 2). Significant differences were detected. Specifically, in the work by Yu et al. (2), the ferrous heme was a mixture of five- and six-coordinate conformations and no evidence for a iron-histidine stretching mode was found (T. G. Spiro, private communication). Furthermore, they reported the Fe—CO stretching mode at 495 cm^{-1} . In contrast, in the work by Deinum et al. (1), the ferrous heme was five-coordinate, the iron-histidine mode was located at 204 cm^{-1} , and the Fe—CO mode at 472 cm^{-1} .

In an attempt to address the differences reported in the resonance Raman spectra, a detailed characterization of an expressed sGC has been performed. The enzyme was expressed as the $\alpha_1\beta_1$ heterodimer using recombinant baculovirus-transfected insect cells. Resonance Raman spectroscopy of this enzyme reveals that the heme of the enzyme exists as a five-coordinate high-spin state in the ferric form, but upon reduction converts to a mixture of five-coordinate high-spin and six-coordinate low-spin configurations. CO- and NO-bound species were also studied. The similarity in the spectral properties of the NO-bound form of the enzyme to that reported previously indicates that despite the clear differences in spectral features, all the enzyme preparations share a common activation mechanism.

EXPERIMENTAL PROCEDURES

Natural abundance nitric oxide (CP grade 99.5%) and carbon monoxide (CP grade 99.5%) were purchased from Matheson. Isotope-labeled species, $^{15}\text{N}^{18}\text{O}$ (99.9%, 99.4%) and $^{13}\text{C}^{18}\text{O}$ (99.5%, 99.4%) were purchased from ICON Inc.

The enzyme was expressed using recombinant baculovirus-transfected cells as described previously (22). The protein was purified using SDS—polyacrylamide gel electrophoresis. Basal enzyme activity was determined to be 0.09 pmol/min/mg . Heme reconstitution was performed under anaerobic conditions by incubating 2 equiv of protoporphyrin-IX with the protein for 15 min at 37°C . The heme reconstituted enzyme was purified by gel filtration to remove the excess heme. The purified reconstituted sGC has a heme content of 1.6 equiv/heterodimer. The enzyme specific activity was determined to be 22.6 pmol/min/mg .

For all the spectroscopic measurements, the samples were dissolved in 40 mM Bis-Tris buffer at pH 7.6 with 1.0 mM DTT. The sample concentration was kept at 8.0 mM. The ferrous form of the enzyme was generated by first purging the sealed Raman cell with nitrogen followed by adding sodium dithionite in a 5-fold excess. CO- and NO-bound species were prepared by adding the appropriate gas to the ferrous enzyme. NO gas was passed through an aqueous solution of sodium hydroxide and a water bottle to eliminate possible acid contamination. Conversion of the enzyme between different states was monitored by optical absorption.

Optical absorption spectra were measured with a Shimadzu UV2100U spectrophotometer. For the Raman experiments, excitation at 413 nm provided by a Spectra Physics 2080 Krypton laser was used. The scattered light was projected onto the entrance slit of a 1.25 m polychromator (Spex) with a 1200 groove/mm grating. The laser line was blocked by

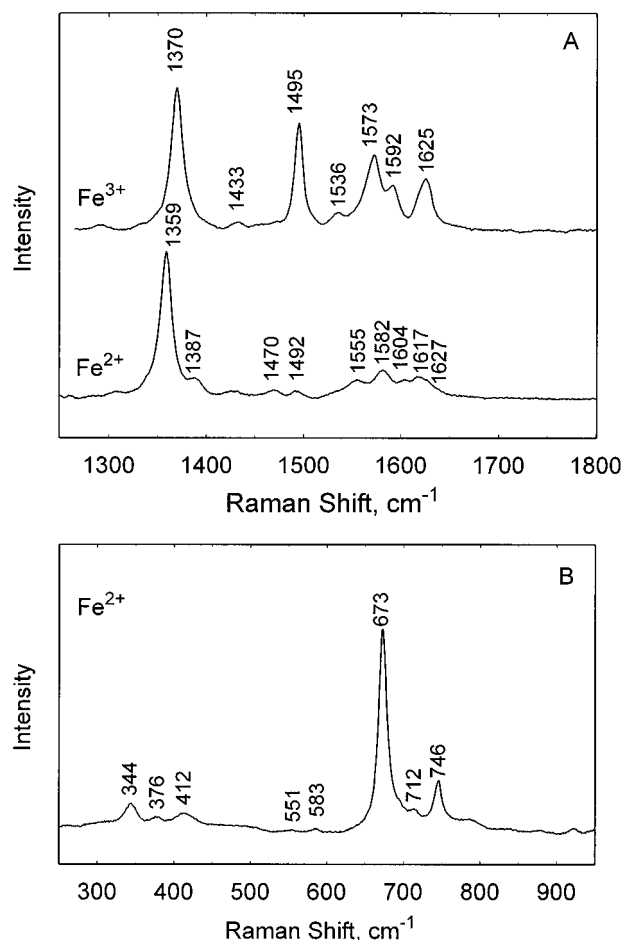


FIGURE 1: Resonance Raman spectra of ligand free sGC. Panel A depicts the spectra in the high-frequency region of the ferric and ferrous forms of the enzyme. Panel B is the low-frequency region of the spectrum of the ferrous enzyme. Spectra for the ferric and ferrous forms were generated with 407 and 413 nm excitation, respectively.

a holographic notch filter in front of the slit. A spectral slit width of 5 cm^{-1} was used. A liquid nitrogen cooled CCD camera (Princeton Instruments) detected the dispersed light. Calibration was performed with lines from neat toluene and an aqueous solution of sodium ferrocyanide. All spectroscopic measurements are performed at room temperature.

Spectral processing was performed using routines provided by Grams 386 (Galactic).

RESULTS

The ferrous form of the enzyme as isolated after reconstitution is stable even under aerobic conditions. It is oxidized to its ferric form only after prolonged exposure to atmospheric oxygen, as indicated by a change in the maximum of the Soret transition from 415 to 390 nm. The resonance Raman spectra of ferric sGC is shown in Figure 1A. The mode (ν_3) at 1495 cm^{-1} is well established as a coordination sensitive marker line. When it is located in the 1480 cm^{-1} region, it signifies that the heme is six-coordinate high spin; when in the $1500\text{--}1505\text{ cm}^{-1}$ region, it indicates that the heme is six-coordinate low spin; and when the line is in the $1490\text{--}1495\text{ cm}^{-1}$ region, it indicates that the heme is five-coordinate high spin. Thus, since ν_3 is located at 1495 cm^{-1} , the data very clearly demonstrate that

Table 1: Comparison of the Primary Resonance Raman Lines Reported for the Ferrous Form of Soluble Guanylate Cyclase^a

source	ν_4	ν_3	ν_{38}	ν_2	ν_{37}	ν_{cc}	ν_{10}	$\nu_{\text{Fe-His}}$
this work	1359	1470/1492	1555	1582	1604	1617	1627	NO ^d
Yu et al. ^b	1360	1468/1493	1557	1584	1604	1618	1626	NO ^d
Deinum et al. ^c	1358	1471	NG ^e	1562	1588	1626	1606	204

^a All frequencies are in wavenumbers (cm^{-1}). ^b Ref 2. ^c Ref 1. ^d Not observed. ^e Not given.

the heme is in a five-coordinate high-spin state, similar to assignments that have been made in other heme proteins (23, 24). The intensity of the line is very high. This is consistent with a five-coordinate high-spin methemoglobin from *Scapharca inaequivalvis* in which this mode is also very strong (25).

The ferrous form of sGC serves as the structural basis for the basal activity of the enzyme. The difference between this state and the NO-bound form can provide understanding of the structural changes associated with the activation of the enzyme. Just as for the ferric oxidation state of heme proteins, ν_3 serves as a coordination state marker line in the ferrous state as well, with five-coordinate high-spin states displaying a frequency at $\sim 1470 \text{ cm}^{-1}$ and low-spin states having a frequency at $\sim 1490 \text{ cm}^{-1}$. Resonance Raman spectra of the ferrous form of sGC in the absence of any added exogenous ligand obtained with 413 nm excitation is shown in Figure 1A. In the high-frequency region, the spectral features show that the heme has contributions from both six-coordinate low-spin and five-coordinate high-spin states, indicated by two lines in the ν_3 region at 1470 and 1492 cm^{-1} . Similar behavior was also observed by Yu et al., who reported a doublet for ν_3 at 1468 and 1493 cm^{-1} (2). Other porphyrin modes of the ferrous enzyme also show similarity to their data as is summarized in Table 1. Although it is clear from our data that our preparation is a mixture, the intensity of the low-spin contributions are quite large. These results are in contrast with the observations by Deinum et al. (1), who observed only a single line for ν_3 at 1471 cm^{-1} in the resonance Raman spectra. Moreover, their high-frequency spectrum is characteristic of a five-coordinate high-spin species, indicating a homogeneous population of a five-coordinate high-spin heme in their ferrous form of the enzyme.

The low-frequency region of the ferrous spectrum confirms the conclusions drawn from the high-frequency region as may be seen in Figure 1B. The spectrum resembles that of a low-spin heme, especially the pattern observed with the three peaks at 344, 376, and 412 cm^{-1} as well as the presence of a line at 746 cm^{-1} . These features are similar to those observed for the low-frequency region of the CO-bound form (Figure 2), except for the absence of the Fe—CO stretching mode (497 cm^{-1}), confirming the contribution from the six-coordinate low-spin heme in the ferrous preparation. Of particular significance is the absence of any line in the 200–230 cm^{-1} region, where the iron-histidine stretching mode ($\nu_{\text{Fe-His}}$) is expected. The $\nu_{\text{Fe-His}}$ mode is only observable for five-coordinate ferrous hemes. These results are in marked contrast with those of Deinum et al. (1), in which a strong $\nu_{\text{Fe-His}}$ was observed at 204 cm^{-1} . Furthermore, their spectra throughout the low-frequency region, which are characteristic of a five-coordinate high-spin heme, are very different from ours, which are characteristic of a six-coordinate low-spin heme.

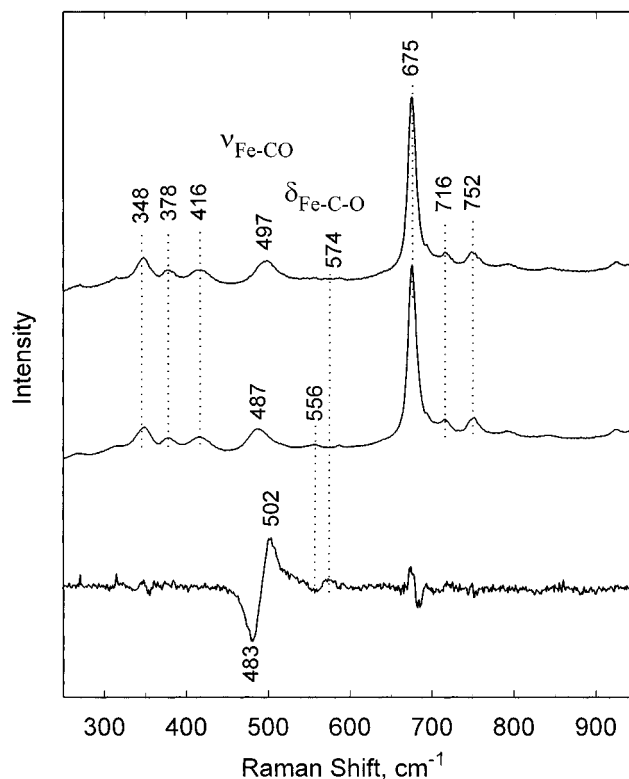


FIGURE 2: Low-frequency region of the resonance Raman spectra of ferrous carbon monoxide bound sGC. Trace A: ferrous enzyme coordinated by natural abundance carbonmonoxide, $^{12}\text{C}^{16}\text{O}$. Trace B: ferrous enzyme coordinated by isotope labeled carbonmonoxide, $^{13}\text{C}^{18}\text{O}$. Trace C: difference spectra between trace A and trace B ($A - B$), showing the isotope effect on the ν_{FeCO} mode. Low excitation power ($\sim 1 \text{ mW}$) and high a rotation rate (2000 rps) was used to avoid possible photolysis. The spectra are the average of several 2 min accumulations with 413 nm excitation. The background was corrected to remove a slight fluorescence.

Table 2: Comparison of the Primary Resonance Raman Lines Reported for the Ferrous Carbonmonoxide Adducts of Soluble Guanylate Cyclase^a

source	ν_4	ν_3	ν_2	ν_{10}	$\nu_{\text{Fe-CO}}$	$\delta_{\text{Fe-C-O}}$	ν_{CO}
this work	1371	1497	1582	1627	497	574	1959
Yu et al. ^b	1370	1499	1584	NG ^d	495	NG ^d	NG ^d
Deinum et al. ^c	1371	1500	1581	1629	472	562	1987 ^e

^a Frequencies are in wavenumbers (cm^{-1}). ^b Ref 2. ^c Ref 1. ^d Not given. ^e Ref 26.

Carbon monoxide forms a stable complex with sGC. Although a spin state mixture was observed for the ferrous form, a single line for ν_3 at 1497 cm^{-1} was observed when the ferrous sample was coordinated by CO, indicating a six-coordinate low-spin homogeneous population (Figure 2). All the other modes are consistent with this assignment. These results for the CO-derivative are similar to those reported by both Yu et al. (2) and Deinum et al. (1), as summarized in Table 2. The carbon-oxygen stretching mode (ν_{CO}) is observed in the high-frequency region at 1959 cm^{-1} with natural abundance CO and shifted to 1866 cm^{-1} when $^{13}\text{C}^{18}\text{O}$ is used (Figure 3). In a previous FT-IR study by Kim et al. (26), this mode was observed at a much higher frequency (1987 cm^{-1}) for sGC.

In the low-frequency region, two other CO isotope sensitive modes are observed at 497 and 574 cm^{-1} (Figure 2). These modes are shifted to 487 and 556 cm^{-1} when the

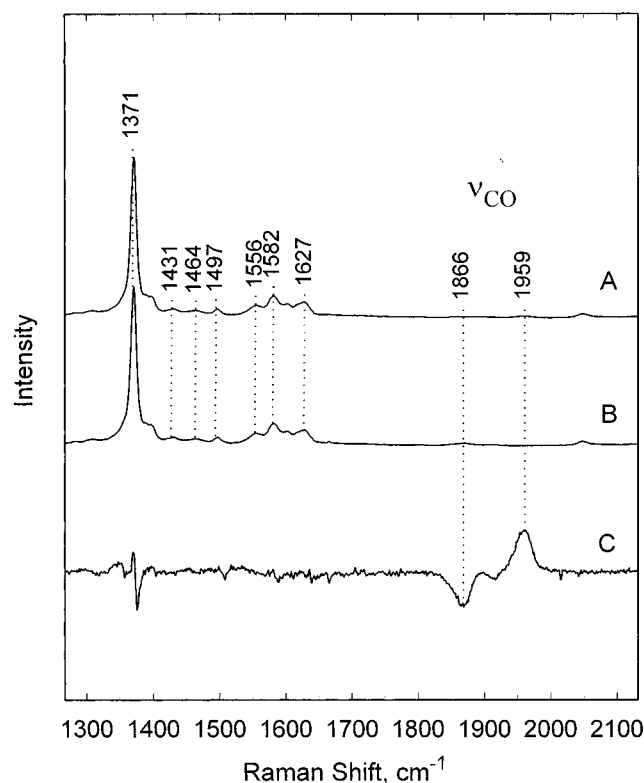


FIGURE 3: High-frequency region of the resonance Raman spectra of the ferrous carbonmonoxide adducts of sGC. Trace A: ferrous enzyme coordinated by natural abundance carbonmonoxide, $^{12}\text{C}^{16}\text{O}$. Trace B: ferrous enzyme coordinated by isotope labeled carbonmonoxide, $^{13}\text{C}^{18}\text{O}$. Trace C: difference spectrum (A - B) showing the assignment of the $\nu_{\text{Fe-CO}}$ mode. The experimental conditions are the same as in Figure 2.

protein is coordinated by $^{13}\text{C}^{18}\text{O}$ and are assigned as the Fe-CO stretching ($\nu_{\text{Fe-CO}}$) and Fe-C-O bending ($\delta_{\text{Fe-C-O}}$) modes, respectively. The $\nu_{\text{Fe-CO}}$ frequency is typical of a six-coordinate low-spin CO complex with histidine proximal ligation (27, 28). For example, this mode is observed at 507 cm^{-1} in sperm whale myoglobin (29) and shifts to the 490–500 cm^{-1} in a variety of mutant myoglobins (30–32). This frequency is also very similar to that observed by Yu et al. (2) at 495 cm^{-1} for sGC, but significantly different from that reported by Deinum et al. (1) at a much lower frequency (472 cm^{-1}). The Fe-C-O bending mode at 574 cm^{-1} falls within the range of a series of heme proteins with histidine proximal ligation (28, 33). This mode was observed for sGC at 562 cm^{-1} by Deinum et al. (1) but was not reported by Yu et al. (2).

Resonance Raman measurements were also made on the Fe-NO-bound enzyme. The most important feature in the high-frequency spectrum is the spin state marker line, ν_3 , occurring at 1508 cm^{-1} (Figure 4A), which indicates five-coordination. This has been observed for other five-coordinate ferrous hemes coordinated by NO as summarized in ref 1 and as detected by them and by Yu et al. (2). All the other spectral features in Figure 4A, including ν_4 (1375 cm^{-1}), ν_2 (1584 cm^{-1}), ν_{10} (1645 cm^{-1}), are identical with those observed by both Yu et al. (2) and Deinum et al. (1) (Table 3), indicating that a similar five-coordinate NO-bound ferrous heme is formed in each case. No isotope-sensitive mode is detectable in the high-frequency region in our data due to the broad shoulder on the line at 1645 cm^{-1} , whereas

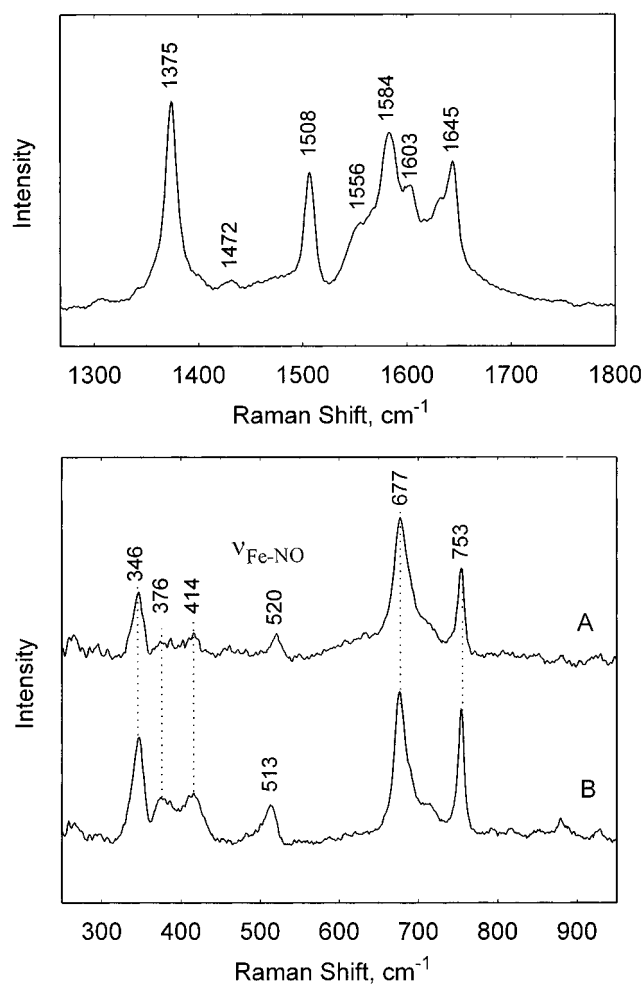


FIGURE 4: Resonance Raman spectra of the ferrous nitric-oxide-bound sGC. The Upper Panel depicts the high-frequency region of NO-bound ferrous sGC. The Lower Panel shows the low-frequency spectra of the ferrous NO-bound enzyme with different isotope labels. Trace A: sGC($\text{Fe}^{2+}/^{14}\text{N}^{16}\text{O}$). Trace B: sGC($\text{Fe}^{2+}/^{15}\text{N}^{18}\text{O}$). Laser excitation at 413 nm was used for data accumulation. All spectra were background corrected.

Table 3: Comparison of the Primary Resonance Raman Lines Reported for the Ferrous Nitric Oxide Adducts of Soluble Guanylate Cyclase^a

source	ν_4	ν_3	ν_2	ν_{10}	$\nu_{\text{Fe-NO}}$	$\delta_{\text{Fe-N-O}}$	ν_{NO}
this work	1375	1508	1584	1645	520	NO ^d	NO ^d
Yu et al. ^b	1376	1508	1585	1646	NO ^d	NO ^d	NO ^d
Deinum et al. ^c	1375	1509	1584	1646	525	NO ^d	1677

^a All line frequencies are in wavenumbers (cm^{-1}). ^b Ref 2. ^c Ref 1. ^d Not observed.

Deinum observed the N-O stretching mode (ν_{NO}) at 1677 cm^{-1} .

In the low-frequency region, an isotope-sensitive line is observed at 520 cm^{-1} with natural abundance NO (Figure 4B). This mode shifts to 513 cm^{-1} with isotope-enriched NO ($^{14}\text{N}^{18}\text{O}$). These frequencies are similar to those reported by Deinum et al. (1).

DISCUSSION

The resonance Raman data of the ferrous states (ligand-free and CO-bound) presented here for the $\alpha_1\beta_1$ form of sGC from baculovirus are very similar to the spectra from the

enzyme reported by Yu et al. (2) but quite different from those reported by Deinum et al. (1). On the other hand, the NO forms of all three preparations are the same. In our recombinant preparation, the heme in the ferric protein is five-coordinate high spin whereas in the ferrous ligand-free form it is primarily six-coordinate low spin. The CO-bound ferrous form has frequencies for the Fe–C–O modes that are similar to other heme proteins but quite distinct from those reported by Deinum et al. (1). Below, we attempt to reconcile the diverse results reported by the three different groups.

The first question to address is what is the proximal ligand in our preparation. For this determination, one normally examines the low-frequency region of the ferrous ligand-free protein. The iron–histidine stretching mode appears for such samples in the 200–230 cm^{-1} region. However, the mode is absent for ferric forms of heme proteins and for six-coordinate ferrous forms. We are unable to detect the characteristic mode since the low-frequency region in our spectrum shows only modes from the six-coordinate species in the ferrous form. Deinum et al. (1), who observed a five-coordinate ferrous form, did detect the iron–histidine mode at 204 cm^{-1} demonstrating that their preparation has a histidine as the proximal ligand.

Examination of the Fe–C–O modes in the resonance Raman spectrum also can reveal the identity of the proximal ligand as the $\nu_{\text{Fe–CO}}$ and ν_{CO} modes can be affected by variety of structural factors, including proximal ligation and distal interactions. The identity of the proximal ligand can be determined by the $\nu_{\text{Fe–CO}}$ and ν_{CO} correlation curve. This well-established correlation curve is distinctly different for proximal ligation by a histidine versus that of a thiolate since the different proximal ligands affect the σ -orbital between the iron and the carbon (28, 34). The $\nu_{\text{Fe–CO}}$ and ν_{CO} frequencies are observed at 497 and 1959 cm^{-1} , respectively, in the present study. Those observed by Deinum et al. (1) show a much lower frequency for $\nu_{\text{Fe–CO}}$ at 472 cm^{-1} and a much higher frequency for ν_{CO} at 1987 cm^{-1} in the FT-IR studies (26). It has been demonstrated by Kim et al. (26) that the ν_{CO} and $\nu_{\text{Fe–CO}}$ fall on the correlation curve for proximal histidine ligation. This is not surprising since $\nu_{\text{Fe–His}}$ itself has been detected in their sample. Interestingly, as shown in Figure 5 the frequencies for ν_{CO} and $\nu_{\text{Fe–CO}}$ found in our samples fall on the same correlation curve for proteins with a histidine proximal ligand. This confirms that the proximal ligand in the enzyme studied here is a histidine, just as in the preparation used in the study of Deinum et al. (1), even though no $\nu_{\text{Fe–His}}$ mode is observed in our case.

In general, in ferric derivatives of heme proteins, the properties of the distal environment control the spin and ligation states; and in the ferrous derivatives the distal environment controls the coordination state and the vibrational frequencies of the Fe–C–O modes in the CO derivatives. When the distal site contains polar residues, water and hydroxide coordinate to the iron in the ferric oxidation state. On the other hand, when bulky residues or a nonpolar pocket is present, the heme remains five-coordinate. If the heme proximal ligand is histidine, the $\nu_{\text{Fe–CO}}$ mode is located in the 490–500 cm^{-1} region for an open pocket without any residues in van der Waals contact with the CO but at higher frequencies when positively charged residues are present and presumably at lower

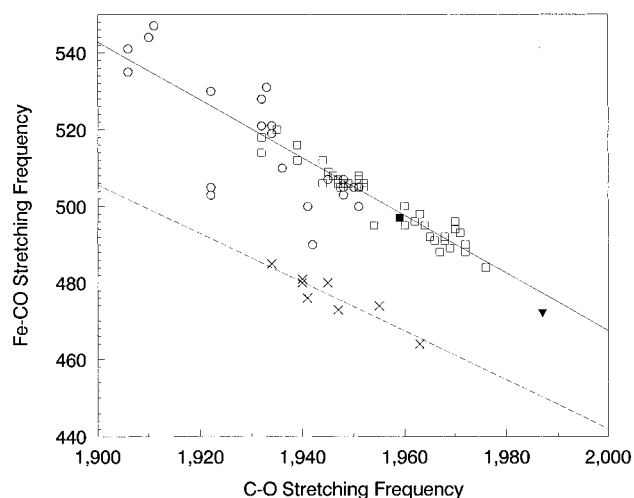


FIGURE 5: Correlation between $\nu_{\text{Fe–CO}}$ and ν_{CO} vibration frequencies in heme proteins. The open squares represent data from samples with proximal histidine ligation (hemoglobins, myoglobins, and porphyrins bound with imidazole). The open circles are data from proteins with imidazolate proximal ligation. The crosses are data from samples with proximal cysteine ligation, e.g., cytochrome P450s. The lines through the data points are least-squares fits of those points. Data from soluble guanylate cyclase are high-lighted for clarity. The solid square is data from this study and the solid inverted triangle is for data from Deinum et al. (1) and Kim et al. (26).

frequencies when negatively charged residues are present (27, 28, 35).

The spectra of our ferric enzyme clearly demonstrate five-coordinate; however, six-coordinate is demonstrated in the ferrous case. We attribute these observations to a nonpolar environment in the distal pocket. This environment prevents coordination of any ligand in the ferric form. On the other hand, the pocket is very open so a ligand, probably exogenous, does coordinate in the ferrous oxidation state. The Fe–C–O modes, which are typical of open pocket heme proteins with proximal histidine coordination, confirms the very open pocket in our preparation. In contrast, in the work of Deinum et al. (1), no significant occupation of the distal pocket is indicated. Thus, no ligand coordinates to the iron in the ferrous “ligand-free” form and the Fe–C–O modes are located at frequencies indicative of very strong interactions with a negatively charged group.

As described above, our data indicate that the distal environment in the preparation of Deinum et al. (1) is very different from that of our preparation [and that of Yu et al. (2)]. However, the proximal bond is the same, although whether or not it has similar strength cannot be determined at present. We now ask how do these differences affect functionality?

Despite the differences observed in the ferrous ligand-free and CO-bound forms of the enzyme, the Fe–NO-bound state of the ferrous heme, which is the active state of the enzyme, is very similar for all three preparations. For example, the modes in the high-frequency region are all the same within 2 cm^{-1} , and in the low-frequency region, we detect the Fe–NO mode at 520 cm^{-1} whereas Deinum et al. (1) report it at 518 cm^{-1} . We view these differences as insignificant and conclude that the structure of the heme in the NO-bound form of the proteins is the same. This is consistent with the biochemical assays on the three different

preparations that all show significant activation upon NO ligation (17, 19, 22). Therefore, the three enzyme preparations most likely share the same mechanism of activation. This should be expected since the proximal ligation is the same in all three cases.

The identity of the sixth ligand in the ferrous form of sGC is difficult to determine at present. However, it must be a ligand that binds more favorably to the ferrous heme as compared to the ferric heme since the latter is five-coordinate. Noting that reduced cytochrome *c*, that has histidine and methionine as axial ligands, is more stable than the oxidized protein points to the possibility of a ligand involving sulfur (36). However, additional experiments are needed to confirm such ligation and to determine if the coordinating ligand is endogenous or exogenous. This is particularly important since the affinity of sGC toward various potential ligands may depend critically on the properties of the distal pocket. The importance of the distal environment in sGC in regulating ligand binding properties has been proposed based on the unique polar effects observed in sGC by Deinum et al. (1) and by Kim et al. (26). They suggest that the decreased binding affinity for O₂, CO, and NO by the increased off-rate characteristic of sGC is due to the steric interactions in the distal pocket.

Finally, we must address the question of why our preparation has spectral properties more similar to those of Yu et al. (2) rather than to those of Deinum et al. (1). In the preparation used by the former, the heme was reconstituted into the enzyme, just as in our preparation, whereas in the preparation of the latter, the heme is retained in the isolation procedure. Recent resonance Raman studies on sGC by Tomita et al. (37) report spectra similar to those of Deinum et al. (1), using the same preparation as they used. This confirms that each of the different protocols of the isolation yield protein with reproducible spectral properties, and since all the preparations are of the same molecular origin, it suggests that the differences in the resonance Raman spectra may be a consequence of heme reconstitution. Efforts are currently underway to reconstitute the enzyme under different conditions in order to clarify the origin of the differences and determine if one of the forms can be converted to the other. Although the spectral differences may result from the differences in the heme incorporation, the presence of different isoforms resulting from the preparations cannot be ruled out. It has been demonstrated that the soluble form of guanylate cyclase has multiple heterodimer isoforms. Since the protein used here was expressed from the cDNAs of each of the subunits, we are confident that we are examining the $\alpha_1\beta_1$ isoform. Isolation from tissue may give a mixture of various subunit compositions. We are currently examining isoforms with different compositions to test this possibility. However, it must be stressed that since the enzyme activity and the NO activation properties of our preparation are similar to those reported by others, the differences in the mode of preparation apparently do not affect the functional properties of the enzyme in a qualitative manner.

REFERENCES

- Deinum, G., Stone, J. R., Babcock, G. T., and Marletta, M. A. (1996) *Biochemistry* 35, 1540–7.
- Yu, A. E., Hu, S., Spiro, T. G., and Burstyn, J. N. (1994) *J. Am. Chem. Soc.* 116, 4117–8.
- Schmidt, H. H., Lohmann, S. M., and Walter, U. (1993) *Biochim. Biophys. Acta* 1178, 153–75.
- Hobbs, A. J., and Ignarro, L. J. (1996) *Methods Enzymol.* 269, 134–48.
- Garbers, D. L., Koesling, D., and Schultz, G. (1994) *Mol. Biol. Cell* 5, 1–5.
- Yuen, P. S. T., and Garbers, D. L. (1992) *Annu. Rev. Neurosci.* 15, 193–225.
- Shyjan, A. W., De Sauvage, F. L., Gillett, N. A., Goeddel, D. V., and Lowe, D. G. (1992) *Neuron* 9, 727–37.
- Traylor, T. G., and Sharma, V. S. (1992) *Biochemistry* 31, 2847–9.
- Stone, J. R., and Marletta, M. A. (1996) *Biochemistry* 35, 1093–9.
- Dierks, E. A. and Burstyn, J. N. (1996) *Biochem. Pharmacol.* 51, 1593–600.
- Schmidt, H. H. W., Pollock, J. S., Nakane, M., Gorsky, L. D., Forstermann, U., and Murad, F. (1991) *Proc. Natl. Acad. Sci. U.S.A.* 88, 365–9.
- Koesling, D., Bohme, E., and Schultz, G. (1991) *FASEB J.* 5, 2785–91.
- Wedel, B., Harteneck, C., Foerster, J., Friebe, A., Schultz, G., and Koesling, D. (1995) *J. Biol. Chem.* 270, 24871–5.
- Harteneck, C., Koesling, D., Soling, A., Schiltz, G., and Bohme, E. (1990) *FEBS Lett.* 292, 217–22.
- Stone, J. R., and Marletta, M. A. (1995) *Biochemistry* 34, 14668–74.
- Foerster, J., Harteneck, C., Malkewitz, J., Schultz, G., and Koesling, D. (1996) *Euro. J. Biochem.* 240, 380–6.
- Burstyn, J. N., Yu, A. E., Dierks, E. A., Hawkins, B. K., and Dawson, J. H. (1995) *Biochemistry* 34, 5896–903.
- Stone, J. R., Sands, R. H., Dunham, W. R., and Marletta, M. A. (1996) *Biochemistry* 35, 3258–62.
- Stone, J. R., and Marletta, M. A. (1994) *Biochemistry* 33, 5636–40.
- Kim, T. D., and Burstyn, J. N. (1994) *J. Biol. Chem.* 269, 15540–5.
- Rousseau, D. L., and Ondrias, M. R. (1984) in *Optical Techniques in Biological Research* Rousseau, D. L., ed. (Academic Press, Orlando, FL).
- Gupta, G., Kim, J., Yang, L., Sturley, S. L., and Danziger, R. S. (1997) *Protein Expression Purif.* 10, 325–330.
- Dasgupta, S., Rousseau, D. L., Anni, H., and Yonetani, T. (1989) *J. Biol. Chem.* 264, 654–662.
- Rousseau, D., and Ching, Y. C. (1989) *J. Biol. Chem.* 264, 7878–81.
- Boffi, A., Takahashi, S., Spagnuolo, C., Rousseau, D. L., and Chiancone, E. (1994) *J. Biol. Chem.* 269, 20437–40.
- Kim, S., Deinum, G., Gardner, M. T., Marletta, M. A., and Babcock, G. T. (1996) *J. Am. Chem. Soc.* 118, 8769–70.
- Li, X. Y., and Spiro, T. G. (1988) *J. Am. Chem. Soc.* 110, 6024–33.
- Ray, G. B., Li, X. Y., Ibers, J. A., Sessler, J. L., and Spiro, T. G. (1994) *J. Am. Chem. Soc.* 116.
- Ramsden, J., and Sppiro, T. G. (1989) *Biochemistry* 28, 3125–8.
- Morikis, D., Champion, P. M., Springer, B. A., and Sligar, S. G. (1989) *Biochemistry* 28, 4791–800.
- Egeberg, K. D., Springer, B. A., Martinis, S. A., Sligar, S. G., Morikis, D., and Champion, P. M. (1990) *Biochemistry* 29, 9783–91.
- Biram, D., Garratt, C. J., and Hester, R. E. (1991) in *Spectroscopy of Biological Molecules* (Hester, R. E., and Girling, R. B., Eds.) pp 433–434, Royal Society of Chemistry, Cambridge, U.K.
- Wang, J., Caughey, W. S., and Rousseau, D. L. (1996) in *Methods in Nitric Oxide Research* (Feelisch, M., and Stamler, J. S., Eds.) pp 427–54, John Wiley and Sons, Chichester.
- Yu, N.-T., and Kerr, E. A. (1988) in *Biological Application of Raman Spectroscopy* (Spiro, T. G., Ed.) Vol. 3, pp 39–95, John Wiley and Sons, New York.

- 35. Kushkuley, B., and Stavrov, S. S. (1996) *Biophys. J.* 70, 1214–1229.
- 36. Pascher, T., Chesick, J. P., Winkler, J. R., and Gray, H. B. (1996) *Science* 271, 1558–60.

- 37. Tomita, T., Ogura, T., Tsuyama, S., Imai, Y., and Kitagawa, T. (1997) *Biochemistry* 36, 10155–60.

BI971934B